Fragment Intrinsic Spins and Fragments' Relative Orbital Angular Momentum in Nuclear Fission

Aurel Bulgac,[1] Ibrahim Abdurrahman,[1] Kyle Godbey,[2] and Ionel Stetcu[3]

[1]*Department of Physics, University of Washington, Seattle, Washington 98195-1560, USA*
[2]*Facility for Rare Isotope Beams, Michigan State University, East Lansing, Michigan 48824, USA*
[3]*Theoretical Division, Los Alamos National Laboratory, Los Alamos, New Mexico 87545, USA*

We present the first fully unrestricted microscopic calculations of the primary fission fragment intrinsic spins and of the fission fragments' relative orbital angular momentum for $^{236}\text{U}^*$, $^{240}\text{Pu}^*$, and ^{252}Cf using the time-dependent density functional theory framework. Within this microscopic approach, free of restrictions and unchecked assumptions and which incorporates the relevant physical observables for describing fission, we evaluate the triple distribution of the fission fragment intrinsic spins and of their fission fragments' relative orbital angular momentum and show that their dynamics is dominated by their bending collective modes in contradistinction to the predictions of the existing phenomenological models and some interpretations of experimental data.

While nuclear fission has been studied for more than eight decades [1], a complete microscopic description based on quantum many-body theory is still lacking. Typical microscopic approaches rely on unverified assumptions and/or strong restrictions, thus rendering the treatment incomplete. Phenomenological models are based on the imagination of their creators rather than rigorous quantum mechanics or direct experimental information. Meitner and Frisch [2] correctly identified the main driver of nuclear fission: namely, the competition between the Coulomb energy and the surface potential energy. The formation of the compound nucleus and its extremely slow shape evolution toward the outer fission barrier is correctly encapsulated by Bohr's compound nucleus concept [3,4]. The saturation properties of nuclei along with the symmetry energy constrain the flow of the nuclear fluid from the moment the compound nucleus is formed until scission, which evolves like an incompressible liquid drop of almost constant local proton-neutron mixture. The spin-orbit interaction and pairing correlations control the finer details on how the emerging fission fragments (FFs) are formed, favoring asymmetric fission yields at low excitation energies [5–8]. The critical theoretical ingredients are thus well-known: the incompressibility of nuclear matter, the symmetry energy strength, the surface tension and the proton charge, the spin-orbit and the pairing correlations' strengths. Only recently, a well-founded formalism free of restrictions that incorporates all of these features has been implemented, and the nonequilibrium character of the nuclear large amplitude collective motion, particularly from the outer saddle to the scission configuration, and the excitation energy sharing mechanism between FFs have been unambiguously proven microscopically [9–11].

The FFs' intrinsic spins have been the subject of old and renewed experimental and theoretical investigations [12–19]. In the 1960s, it was conjectured that the emerging FFs acquire intrinsic spins due to the existence of several collective FF spin modes: the double-degenerate transversal modes, wriggling and bending, and the longitudinal modes, twisting and tilting. The origin of the relative orbital angular momentum between fragments has never been elucidated within a fully microscopic framework. Consider the clean case of spontaneous fission of ^{252}Cf from its ground state with $S_0^\pi = 0^+$. The final three angular momenta satisfy the conservation law

$$S_0 = S^L + S^H + \Lambda = 0 \text{ in the case of } {}^{252}\text{Cf,} \quad (1)$$

where $S^{L,H}$ are the FF intrinsic spins and Λ is the FFs' relative orbital angular momentum, which is an integer. Classically, these three vectors lie in a plane, and $\Lambda = R \times P$ is perpendicular to the fission direction, where R, P are the FFs' relative separation and momentum. On its way to scission, this nucleus elongates along a spontaneously broken symmetry direction and the fledging FFs emerge. The longer the nuclear elongation, the larger the moment of inertia of the entire nuclear system is, and the overall rotational frequency controlled by Λ is slower. As FFs emerge, being by nature nonspherical, they rotate with intrinsic spins S^L and S^H, while at the same time they also rotate as a dumbbell around their common center of mass with the angular momentum Λ. Until scission, these three angular momenta can vary subject to restriction Eq. (1). After scission, when the mass and energy exchange between emerging FFs stops, these angular momenta cease to evolve in time (apart from small effects of the Coulomb interaction

between FFs [12,20]). Before scission, the FF identities are not well-defined because matter, momentum, and energy are flowing between them. The FF intrinsic spins and $\mathbf{\Lambda}$ are well-defined only at a sufficiently relative large separation. Even though the initial nuclear system ^{252}Cf has a vanishing initial spin $S_0^\pi = 0^+$, the FFs emerge as wave packets of deformed nuclei, characterized by rotation and vibrational bands. Similar to the well-known bicycle wheel classroom physics demos [21], the dynamics of a spontaneously fissioning ^{252}Cf resembles the dynamics of an instructor on a freely rotating stand ($\mathbf{\Lambda}$) holding two bicycle wheels ($\mathbf{S}^{L,H}$) and is nothing like a "snapping rubber band" [16], which does not rotate.

We use the time-dependent density functional theory (TDDFT) extended to superfluid systems (see recent reviews [22,23] and Refs. [9–11,17]) to determine the triple probability distribution $P(S^L, S^H, \Lambda)$, $\sum_{S^{L,H},\Lambda} P(\Lambda, S^L, S^H) = 1$, by performing a triple angular momenta projection of the overlap [24],

$$\langle\Phi|\Phi(\beta_0,\beta_L,\beta_H)\rangle = \langle\Phi|e^{i\beta_0(J_x^L+J_x^H)}e^{i\beta^L J_x^L}e^{i\beta^H J_x^H}|\Phi\rangle, \quad (2)$$

where Oz is the fission axis and the magnitudes of the angular momenta satisfy the triangle restriction

$$|S^L - S^H| \leq \Lambda \leq S^L + S^H \quad (3)$$

and $|\Phi\rangle$ is the fissioning nucleus intrinsic wave function. In the case of ^{236}U* and ^{240}Pu*, the initial spin $S_0 \neq 0$ and then $|\mathbf{\Lambda} - S_0| = |\mathbf{S}^L + \mathbf{S}^H|$, and since $S_0 \ll \langle\Lambda\rangle$, then $\Lambda \approx |\mathbf{S}^L + \mathbf{S}^H|$ with good accuracy. We determined the probability distribution $p(\cos\phi^{LH})$, where ϕ^{LH} is the angle between S^L and S^H, by constructing a histogram of the expectation of the cosine between

$$\cos\phi^{LH} = \frac{\Lambda(\Lambda+1) - S^L(S^L+1) - S^H(S^H+1)}{2(S^L+1/2)(S^H+1/2)}, \quad (4)$$

where we used the Langer correction [25] in the denominator. Note that the relative angle ϕ^{LH} does not depend on a lab or body reference frame. Optimally, one should consider also an additional projection to enforce the value of total angular momentum $\mathbf{S}_0$, with the rotation operator $P_0 = e^{i\gamma(J_x^L+J_x^H+\Lambda_x)}$, where Λ_x rotates the entire system around its center of mass, a procedure that is expected to lead only to minor corrections [17]. We replaced this projection with the equivalent triangle restriction

$$\triangle = \Theta(\Lambda \geq |S^L - S^H|)\Theta(\Lambda \leq S^L + S^H). \quad (5)$$

We performed TDDFT fission calculations of ^{236}U, ^{240}Pu, and ^{252}Cf using two different nuclear energy density functionals (NEDFs), SkM* [26] and SeaLL1 [27], in simulation boxes $30^2 \times 60$ with a lattice constant and $l = 1$ fm and a corresponding momentum cutoff $p_{\text{cut}} = \pi\hbar/l \approx 600$ MeV/c, and using the LISE package

as described in Refs. [9,11,28]. The excitation energies for ^{236}U and ^{240}Pu were chosen close to the neutron threshold, thus emulating the reactions ^{235}U(n_{th}, f) and ^{239}Pu(n_{th}, f). The initial nuclear wave function $|\Phi\rangle$ was evolved in time from various initial deformations Q_{20} and Q_{30} of the mother nucleus near the outer saddle until the FFs were separated by more than 30 fm as in Refs [10,11,17] and their shapes relaxed. In the case of ^{252}Cf(sf), we started the simulation outside the barrier for energies close to the ground state energy. The current implementation of the TDDFT framework [22,23] has proven capable of providing answers to a wide number of problems in cold atom physics, quantum turbulence in fermionic superfluids, vortex dynamics in neutron star crust, nuclear fission, and reactions. Density functional theory and Schrödinger descriptions are mathematically identical quantum many-body frameworks for one-body densities [29–31], with the proviso that in nuclear physics neither NEDF nor the internucleon forces are known with sufficient accuracy [32].

The distributions of the FFs' orbital angular momenta (see Fig. 1) are the first unrestricted microscopic extractions of these quantities. As the masses of ^{236}U, ^{240}Pu, and ^{252}Cf are close to one another, the Λ distributions obtained by performing a single angular projection of the overlap $\langle\Phi|\Phi(\beta_0)\rangle = \langle\Phi|e^{i\beta_0(J_x^L+J_x^H)}|\Phi\rangle$, as in Ref. [17], are very similar. Such individual intrinsic spin distributions can be recovered independently from our triple projection results from $P(\Lambda, S^L, S^H)$ as follows,

$$P(S^{L,H}) = \sum_{S^H \text{ or } S^L,\Lambda} P(\Lambda, S^L, S^H), \quad \sum_{S^{L,H}} P(S^{L,H}) = 1, \quad (6)$$

$$P(\Lambda) = \sum_{S^{L,H}} P(S^{L,H}), \quad \sum_\Lambda P(\Lambda) = 1, \quad (7)$$

and a comparison between results using the single and the triple projections in case of induced fission of ^{252}Cf are shown in Fig. 2. The more precise triple projection leads to larger FF intrinsic spins by about $2\ldots3\hbar$, while the average orbital angular momentum Λ decreases by about $1\hbar$. (Similar corrections to the FF intrinsic spins would be required for the estimates presented in Ref. [18].) As demonstrated in Ref. [33], the emission of neutrons and statistical gammas reduces the FF spins by $\approx 3.5 - 5\hbar$ by the time the FF decay reaches the yrast bandhead, corresponding to the FF spin values measured by Wilson et al.[16]. The sum of the yrast bandhead spins [16] for ^{252}Cf, $6.85\hbar$ for heavy FF and $6.44\hbar$ for light FF, respectively, (averaged over all measured FFs) with the angular momentum loss to decay 3.5–5$\hbar$ estimated in Ref. [33], using standard phenomenological inputs, however, agrees reasonably well with our estimates of the average intrinsic FF spins in Fig. 2.

In Fig. 3, we show the triple distribution $P(\Lambda, S^L, S^H)$ for odd values of Λ. The even values of Λ fixes both FF parities
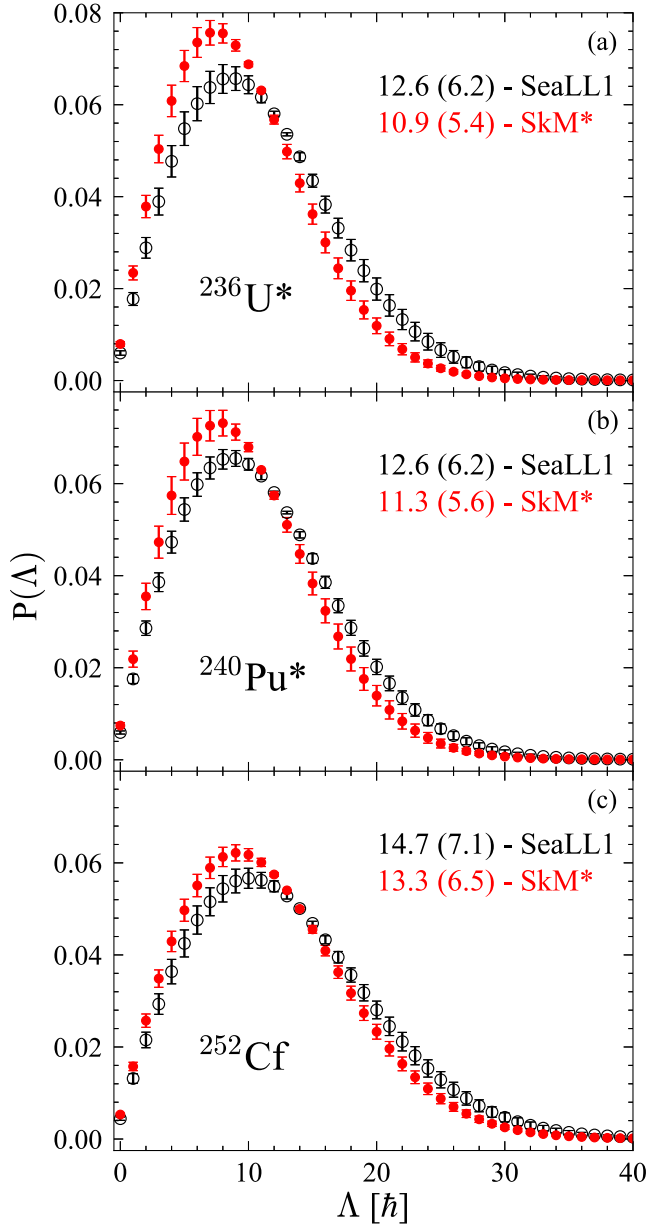
FIG. 1. The orbital angular momentum distribution for three actinides. For each nucleus, the average and the corresponding standard deviations are shown in the legend. The "uncertainties" are the standard deviations that characterize the range of the variations due to the spread of the initial values of the multipole moments Q_{20} and Q_{30} and the energies of the fissioning nucleus [9–11,17] and thus these distributions are characteristics for average FF splittings.

to be identical, $\pi^L = \pi^H$, while in case of odd Λ these parities are opposite, $\pi^L = -\pi^H$, since for ^{252}Cf $S_0^\pi = 0^+$. The distribution $P(\Lambda, S^L, S^H)$ is nonvanishing only in the region defined by Eq. (3).

The distribution of the angles between the intrinsic spins S^L and S^H is particularly instructive and qualitatively different from previous predictions. It was assumed a
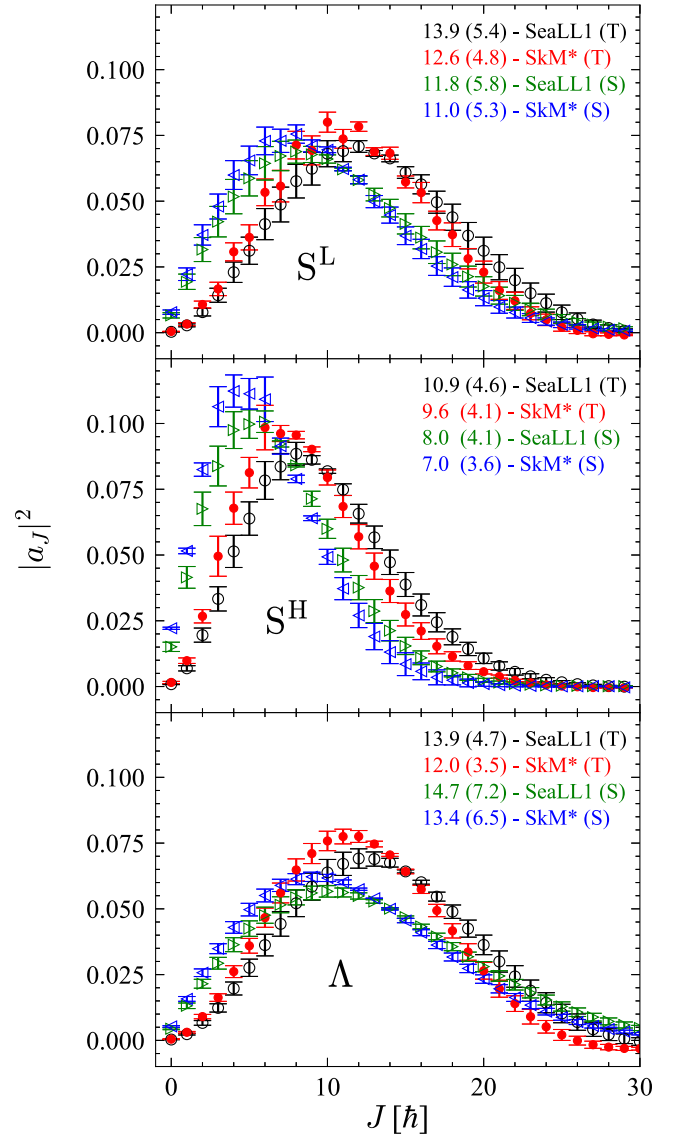
FIG. 2. The light and heavy FF intrinsic spins and the orbital angular momentum distributions in case of spontaneous fission of ^{252}Cf using the triple projection distributions from Eqs. (6), (7) [24] and from the single projection of the FF intrinsic spins [17] and of the orbital angular momentum Λ and the corresponding average values for the intrinsic spin or the orbital angular momentum (standard deviation). (T) and (S) stand for the triple and single projections of the angular momenta.

number of times in the literature (see Refs. [19,34] and references therein) that the two intrinsic spins are very weakly correlated at most. In particular, this was one of the main interpretations of the experimental results recently published by Wilson *et al.* [16]. If that were the case, the distribution $p(\phi^{LH})$ would basically be flat, similar to the predictions in Refs. [19,34], with those results reproduced in this figure. In Fig. 4, the distribution $p(\phi^{LH})$ evaluated by us is clearly not a uniform distribution, with a prominent maximum at an angle $\phi^{LH} \approx 2\pi/3$ [35]. The probability of
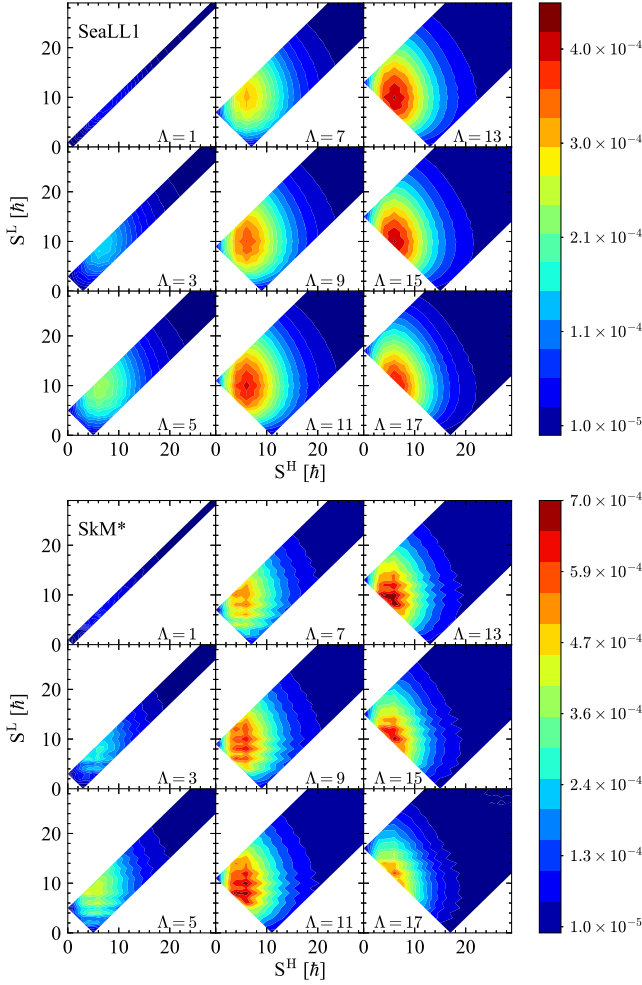
FIG. 3. The ^{252}Cf triple probability distribution $P(\Lambda, S^L, S^H)$ for SeaLL1 (upper panel) and SkM* (lower panel) NEDFs for odd values of Λ. The FF parities are correlated with the orbital angular momentum $\pi^L \pi^H = (-1)^\Lambda$. This triple distribution vanishes outside the region $|S^L - S^H| \le \Lambda \le S^L + S^H$, shown with white in these plots. The distributions for ^{236}U* and ^{240}Pu* are very similar.

FIG. 4. The circles and bullets represent the histogram (bin size = 0.22 radian) of the angle between the FF intrinsic spins S^L and S^H extracted using the triple distribution $P(\Lambda, S^L, S^H)$ and Eq. (4) to evaluate $p(\phi^{LH})$, $\int_0^\pi d\phi^{LH} p(\phi^{LH}) = 1$. The triangles represent the histogram obtained with $P(\Lambda)P(S^L)P(S^H)\triangle$; see text and Eqs. (5), (6). The blue line and diamonds are the prediction of the FREYA model [19]. The distributions $p(\phi^{LH})$ for ^{236}U* and ^{240}Pu* are very similar.

$$\sum_{S^{L,H},\Lambda} |P(\Lambda)P(S^L)P(S^H)\triangle - P(\Lambda, S^L, S^H)| = 0.35, \quad (8)$$

when the geometrical constraint is taken into account.

In Fig. 4, we plot the recent published results obtained with the phenomenological model FREYA, where Randrup and Vogt [19] discussed the generation of the fragment angular momentum in fission. In Ref. [19], the claim is made that, unlike the conclusion reached by [16], i.e., that the FF intrinsic spins were formed after scission and are uncorrelated, the primordial intrinsic spins emerge uncorrelated before scission. This argument is based on the assumptions that the FF spins' dynamics is governed by the rotational energy

$$E_{\text{rot}} = \frac{S^L \cdot S^L}{2I^L} + \frac{S^H \cdot S^H}{2I^H} + \frac{\Lambda \cdot \Lambda}{2I^R}, \quad (9)$$

where $I^{L,H,R}$ are the FFs and orbital moments of inertia, satisfying the relation $I^R \approx 10 I^{L,H}$. The only correlation between $S^{L,H}$ is due to the third term, which is quantitatively small and which one can hardly quantify as highly correlated, and is in stark contradistinction with our microscopic results in the same figure. While at first glance this assumption appears valid (see also Refs. [15,34]), upon closer analysis it becomes clear that the most general form allowed by symmetry is

$$E_{\text{rot}} = (S^L, S^H, \Lambda)^T \otimes \overleftrightarrow{I} \otimes (S^L, S^H, \Lambda), \quad (10)$$

with a nondiagonal 3×3 effective inertia tensor $\overleftrightarrow{I}$ in general.

having angles $\phi^{LH} \ge \pi/2$ is $\approx 0.71/0.72$ (SeaLL1/SkM*), which means that the two FF intrinsic spins are predominantly pointing in opposite directions and that the bending modes are predominantly favored over the wriggling modes. In Fig. 4, we used, instead of the correlated evaluated distribution $P(\Lambda, S^L, S^H)$, the uncorrelated distribution $P(\Lambda)P(S^L)P(S^H)\triangle$ obtained using Eqs. (6), (7), shown with triangles. The results appear very similar, even though $P(\Lambda, S^L, S^H)$ is drastically different from $P(\Lambda)P(S^L)P(S^H)\triangle$, and in evaluating the distribution $p(\theta_{LH})$ we have imposed the Eq. (3) restriction and renormalized the distribution $P(\Lambda)P(S^L)P(S^H)\triangle$ by a (not shown) factor, ≈ 0.74. Figure 4 unfortunately does not reveal the large amount of FF intrinsic spin correlations, which are not merely geometrical in nature, since
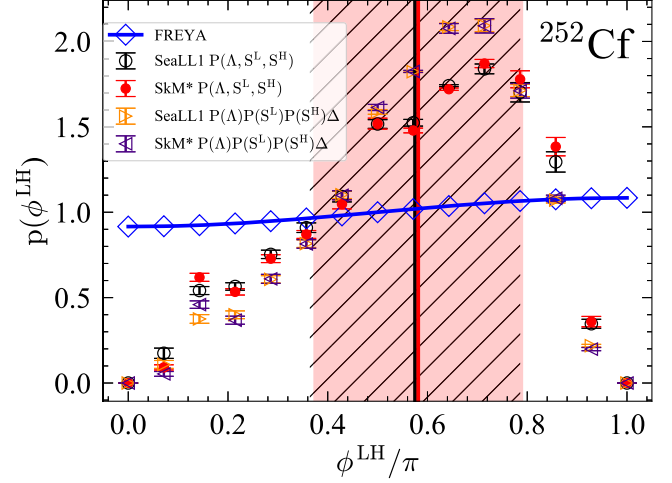
The impact of the emission of neutrons and γ rays on the spin of the FFs was discussed in Ref. [33] within the Hauser-Feshbach framework [36], where it was demonstrated that the intrinsic FF spins can be changed on average by 3.5–5$\hbar$, a process that leads to a strong decorrelation of the observed FF spins, strongly underestimated by the analysis of Ref. [16]. The experimental data [16] characterizes only the yrast bandhead FF spins after a large amount of the internal FF excitation energy, ≈ 20 MeV per FF [9–11,37–39], was carried away by emitted particles. The work presented here can better guide phenomenological models [19,34,38,40] and further extend the analysis in Ref. [33], which all rely on a quite large number of phenomenological parameters.

[1] O. Hahn and F. Strassmann, Über den Nachweis und das Verhalten der bei der Bestrahlung des Urans mittels Neutronen entstehenden Erdalkalimetalle, Naturwissenschaften **27**, 11 (1939).

[2] L. Meitner and O. R. Frisch, Disintegration of uranium by neutrons: A new type of nuclear reaction, Nature (London) **143**, 239 (1939).

[3] N. Bohr, Neutron capture and nuclear constitution, Nature (London) **137**, 344 (1936).

[4] N. Bohr and J. A. Wheeler, The mechanism of nuclear fission, Phys. Rev. **56**, 426 (1939).

[5] V. M. Strutinsky, Shell effects in nuclear masses and deformation energies, Nucl. Phys. **A95**, 420 (1967).

[6] M. Brack, J. Damgaard, A. S. Jensen, H. C. Pauli, V. M. Strutinsky, and C. Y. Wong, Funny hills: The shell-correction approach to nuclear shell effects and its applications to the fission process, Rev. Mod. Phys. **44**, 320 (1972).

[7] G. Bertsch, The nuclear density of states in the space of nuclear shapes, Phys. Lett. **95B**, 157 (1980).

[8] G. F. Bertsch and A. Bulgac, Comment on "Spontaneous Fission: A Kinetic Approach", Phys. Rev. Lett. **79**, 3539 (1997).

[9] A. Bulgac, P. Magierski, K. J. Roche, and I. Stetcu, Induced Fission of ^{240}Pu within a Real-Time Microscopic Framework, Phys. Rev. Lett. **116**, 122504 (2016).

[10] A. Bulgac, S. Jin, K. J. Roche, N. Schunck, and I. Stetcu, Fission dynamics of ^{240}Pu from saddle to scission and beyond, Phys. Rev. C **100**, 034615 (2019).

[11] A. Bulgac, S. Jin, and I. Stetcu, Nuclear fission dynamics: Past, present, needs, and future, Front. Phys. **8**, 63 (2020).

[12] V. M. Strutinsky, Angular anisotropy of gamma quanta that accompany fission, Sov. Phys. JETP **10**, 613 (1960), http://www.jetp.ras.ru/cgi-bin/e/index/e/10/3/p613?a=list.

[13] T. Ericson, The statistical model and nuclear level densities, Adv. Phys. **9**, 425 (1960).

[14] J. R. Nix and W. J. Swiatecki, Studies in the liquid-drop theory of nuclear fission, Nucl. Phys. **71**, 1 (1965).

[15] L. G. Moretto and R. P. Schmitt, Equilibrium statistical treatment of angular momenta associated with collective modes in fission and heavy-ion reactions, Phys. Rev. C **21**, 204 (1980).

[16] J. N. Wilson *et al.*, Angular momentum generation in nuclear fission, Nature (London) **590**, 566 (2021).

[17] A. Bulgac, I. Abdurrahman, S. Jin, K. Godbey, N. Schunck, and I. Stetcu, Fission Fragment Intrinsic Spins and Their Correlations, Phys. Rev. Lett. **126**, 142502 (2021).

[18] P. Marević, N. Schunck, J. Randrup, and R. Vogt, Angular momentum of fission fragments from microscopic theory, Phys. Rev. C **104**, L021601 (2021).

[19] J. Randrup and R. Vogt, Generation of Fragment Angular Momentum in Fission, Phys. Rev. Lett. **127**, 062502 (2021).

[20] A. Bulgac, Fission-fragment excitation energy sharing beyond scission, Phys. Rev. C **102**, 044609 (2020).

[21] Physics demo, http://youtube.com/watch?v=ISImuPcmiC4.

[22] A. Bulgac, Time-dependent density functional theory and the real-time dynamics of fermi superfluids, Annu. Rev. Nucl. Part. Sci. **63**, 97 (2013).

[23] A. Bulgac, Time-dependent density functional theory for fermionic superfluids: from cold atomic gases, to nuclei and neutron star crust, Phys. Status Solidi B **256**, 1800592 (2019).

[24] A. Bulgac, Restoring broken symmetries for nuclei and reaction fragments, Phys. Rev. C **104**, 054601 (2021).

[25] R. E. Langer, On the connetion formulas and the solutions of the wave equation, Phys. Rev. **51**, 669 (1937).

[26] J. Bartel, P. Quentin, M. Brack, C. Guet, and H.-B. Håkansson, Towards a better parametrisation of Skyrme-like effective forces: A critical study of the SkM force, Nucl. Phys. **A386**, 79 (1982).

[27] A. Bulgac, M. M. Forbes, S. Jin, R. N. Perez, and N. Schunck, Minimal nuclear energy density functional, Phys. Rev. C **97**, 044313 (2018).

[28] S. Jin, K. J. Roche, I. Stetcu, I. Abdurrahman, and A. Bulgac, The LISE package: Solvers for static and time-dependent superfluid local density approximation equations in three dimensions, Comput. Phys. Commun. **269**, 108130 (2021).

[29] R. M. Dreizler and E. K. U. Gross, *Density Functional Theory: An Approach to the Quantum Many–Body Problem* (Springer-Verlag, Berlin, 1990).

[30] *Time-Dependent Density Functional Theory*, edited by M. A. L. Marques, C. A. Ullrich, F. Nogueira, A. Rubio, K. Burke, and E. K. U. Gross, Lecture Notes in Physics Vol. 706 (Springer-Verlag, Berlin, 2006).

[31] *Fundamentals of Time-Dependent Density Functional Theory*, edited by M. A. L. Marques, N. T. Maitra, F. M. S. Nogueira, E. K. U. Gross, and A. Rubio, Lecture Notes in Physics Vol. 837 (Springer, Heidelberg, 2012).

[32] G. Salvioni, J. Dobaczewski, C. Barbieri, G. Carlsson, A. Idini, and A. Pastore, Model nuclear energy density functionals derived from ab initio calculations, J. Phys. G **47**, 085107 (2020).

[33] I. Stetcu, A. E. Lovell, P. Talou, T. Kawano, S. Marin, S. A. Pozzi, and A. Bulgac, Angular Momentum Removal by Neutron and γ-Ray Emissions During Fission Fragment Decays, Phys. Rev. Lett. **127**, 222502 (2021).

[34] R. Vogt and J. Randrup, Angular momentum effects in fission, Phys. Rev. C **103**, 014610 (2021).

[35] A. Bulgac, The angular correlation between the fission fragment intrinsic spins, arXiv:2108.07268.

[36] W. Hauser and H. Feshbach, The inelastic scattering of neutrons, Phys. Rev. **87**, 366 (1952).

[37] K.-H. Schmidt and B. Jurado, Review on the progress in nuclear fission—experimental methods and theoretical descriptions, Rep. Prog. Phys. **81**, 106301 (2018).

[38] P. Talou, I. Stetcu, P. Jaffke, M. E. Rising, A. E. Lovell, and T. Kawano, Fission fragment decay simulations with the CGMF code, Comput. Phys. Commun. **269**, 108087 (2021).

[39] J. Randrup and R. Vogt, Calculation of fission observables through event-by-event simulation, Phys. Rev. C **80**, 024601 (2009).

[40] B. Becker, P. Talou, T. Kawano, Y. Danon, and I. Stetcu, Monte Carlo Hauser-Feshbach predictions of prompt fission γ rays: Application to $n_{th} + {}^{235}U$, $n_{th} + {}^{239}Pu$, and ${}^{252}Cf$ (sf), Phys. Rev. C **87**, 014617 (2013).